

This is an Open Access document downloaded from ORCA, Cardiff University's institutional repository: <https://orca.cardiff.ac.uk/id/eprint/117750/>

This is the author's version of a work that was submitted to / accepted for publication.

Citation for final published version:

Chappell, Adrian , Webb, Nicholas P., Leys, John F., Waters, Cathy, Orgill, Susan and Eyres, Michael 2019. Minimising soil organic carbon erosion by wind is critical for land degradation neutrality. *Environmental Science and Policy* 93 10.1016/j.envsci.2018.12.020

Publishers page: <https://doi.org/10.1016/j.envsci.2018.12.020>

Please note:

Changes made as a result of publishing processes such as copy-editing, formatting and page numbers may not be reflected in this version. For the definitive version of this publication, please refer to the published source. You are advised to consult the publisher's version if you wish to cite this paper.

This version is being made available in accordance with publisher policies. See <http://orca.cf.ac.uk/policies.html> for usage policies. Copyright and moral rights for publications made available in ORCA are retained by the copyright holders.



Minimising soil organic carbon erosion by wind is critical for land degradation neutrality.

Adrian Chappell¹, Nicholas P. Webb², John F. Leys³, Cathy Waters⁴, Susan Orgill⁵ and Michael Eyres⁶

¹*School of Earth and Ocean Sciences, Cardiff University, Wales, CF10 3AT UK.*

²*USDA-ARS Jornada Experimental Range, Las Cruces, NM, USA.*

³*Knowledge Services Team, Science Division, NSW Environment and Heritage, Gunnedah, Australia.*

⁴*NSW Department of Primary Industries, PMB 19 Trangie NSW 2823 Australia.*

⁵*NSW Department of Primary Industries, Pine Gully Road, Wagga Wagga NSW 2650 Australia.*

⁶*Injekta Field Systems, Kent Town, SA, Australia.*

Abstract

The Land Degradation-Neutrality (LDN) framework of the United Nations Convention to Combat Desertification (UNCCD) is underpinned by three complementary interactive indicators (metrics: vegetation cover, net primary productivity; NPP and soil organic carbon; SOC) as proxies for change in land-based natural capital. The LDN framework assumes that SOC changes slowly primarily by decomposition and respiration of CO₂ to the atmosphere. However, there is growing evidence that soil erosion by wind, water and tillage also reduces SOC stocks rapidly after land use and cover change. Here we modify a physically-based sediment transport model to estimate wind erosion and better represent the vegetation cover (using land surface aerodynamic roughness; that is the plant canopy coverage, stone cover, soil aggregates, etc. that protects the soil surface from wind erosion) and quantify the contribution of wind erosion to global SOC erosion (2001-2016). We use the wind erosion model to identify global dryland regions where SOC erosion by wind may be a significant problem for achieving LDN. Selected sites in global drylands show SOC erosion by wind accelerating over time. Without targeting and reducing SOC erosion, management practices in these regions will fail to sequester SOC and reduce land degradation. We describe the interrelated nature of the LDN indicators, the importance of including SOC erosion by wind erosion and how by explicitly accounting for wind erosion processes, we can better represent the physical effects of changing land cover on land degradation. Our results for Earth's drylands show that modelling SOC stock reduction by wind erosion is better than using land cover and SOC independently. Furthermore, emphasising the role of wind erosion in UNCCD and Intergovernmental Panel on Climate Change (IPCC) reporting will better support LDN and climate change mitigation and adaptation globally.

Keywords: Land degradation neutrality; Soil organic carbon; Land cover; Wind erosion; Sequestration;

Introduction

Humans have substantially impacted the Earth's surface via land cover change (LCC) associated with widespread land use change (LUC) and an intensification of land management practices (Luyssaert et al., 2014). Early agriculture exploited the soil's natural balance of inputs and losses of nutrients and soil organic carbon (SOC) to feed a rapidly expanding global population (Amundsen et al., 2015; Figure 1). However, in many regions agriculture has accelerated the loss of fertile topsoil by wind, water and tillage erosion to orders of magnitude greater than soil formation (Amundson et al., 2015; Figure 1). This reduces soil nutrient capacity and soil profile water content, thus representing a major threat to the productive potential of landscapes (FAI & ITPS, 2015). Accelerated soil erosion changes every biophysical and biogeochemical cycle, perturbing the cycles of C, dust,

energy and water and degrades soil and air quality which impact global socio-economic systems. Soil erosion therefore represents one of the most important and highly synergistic processes of land degradation. For example, the loss of soil by wind erosion reduces the depth of soil and its potential to support agricultural production (Webb et al., 2017). Wind erosion also causes dust emission and the preferential removal of fine, C- and nutrient-rich material (Chappell et al., 2013). Vegetation species change in response to the redistribution and loss of soil nutrients and possible changes in soil hydrology. Typically, as vegetation cover declines, the sheltering of bare surfaces is reduced causing wind erosion to accelerate. Such feedbacks can be a key driver of regional ecosystem change (Bestelmeyer et al., 2015).

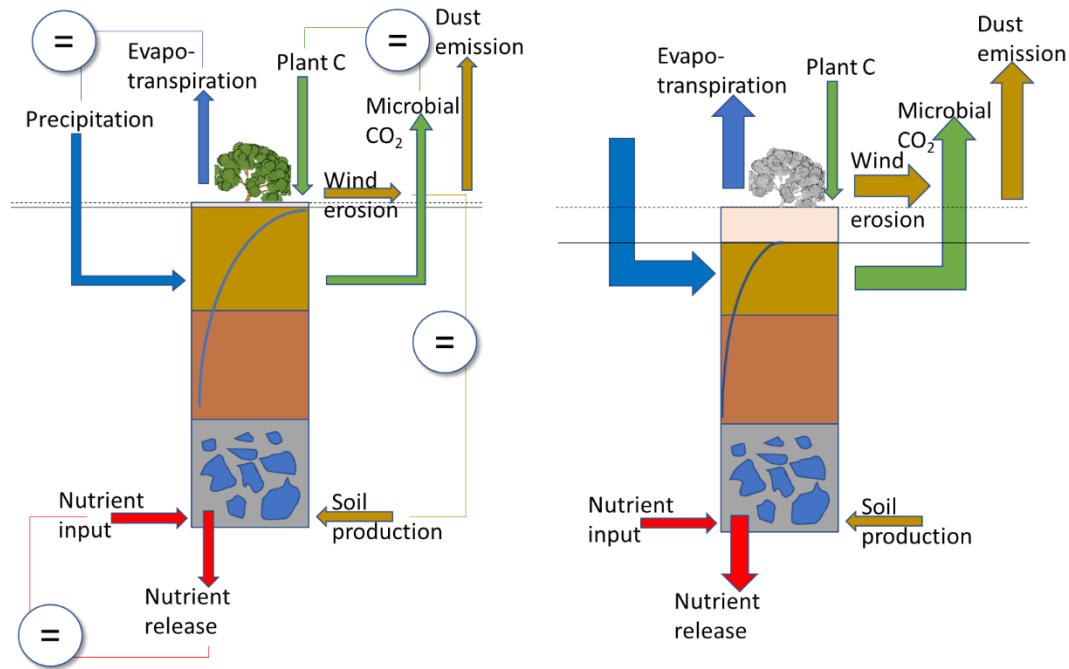


Figure 1. Steady states (=) in Earth's systems are perturbed by human activity causing accelerated soil erosion which feedback and interact (synergistic) to changes in the biophysical and biogeochemical cycles, altering system balance (adapted from Amundsen et al., 2015).

Wind and water erosion influence the flux and stock of SOC lost from soil in several ways. There is considerable debate about the fate of SOC removed by soil erosion with some studies suggesting it may be dynamically replaced (Stallard 1998), protected after deposition (Van Oost *et al.* 2007) thereby representing a potential C sink (Dialynas *et al.* 2016), or more exposed to mineralisation during erosion and transport (Lal 2004; Lal 2005) which may change the prevailing chemistry of the eroded OM (Ellerbrock *et al.* 2016; Sommer *et al.* 2016). Organic matter is preferentially removed from soil during erosion due to its low density and this primarily occurs at the soil surface (with the exception of gully and rill erosion) where the concentration of OC is greatest (Gregorich *et al.* 1998; Lal 2003). Consequently, eroded sediment is estimated to be up to five times more enriched with OC than most topsoil (Lal 2003). Organic matter in eroded sediment is then more vulnerable to mineralisation through direct exposure and oxidation, or through the degradation of aggregates where OM is occluded (Lal 2003; Lal 2005; Nguyen *et al.* 2008). Wind erosion degrades macroaggregates thereby accelerating OM mineralisation (Elliott 1986; Li *et al.* 2014; Singh and Singh 1996). Furthermore, large dust emission events may transport fine eroded sediment (e.g., less than 22 μm) offshore (Leys *et al.* 2011) thereby representing a loss of C from the terrestrial system (Chappell *et al.* 2013).

About 11% of the Earth's land surface is agricultural land, of which 80% suffers moderate erosion (Pimentel, 1993). Since farming began, an area greater than the Earth's cropland has been abandoned due to erosion (Lal, 1990). The total economic value of erosion-induced loss is estimated at USD400 billion per year from arable land alone (FAO & ITPS, 2015) and some 10 million ha of cropland worldwide is abandoned each year due to soil erosion (Faeth and Crosson, 1994). The World Health Organisation (WHO) reported more than 3.7 billion people worldwide are malnourished (WHO, 2004). The vast majority of affected developing countries are in drylands

73 where soil erosion is greatest. If accelerated erosion continues unabated, yield reduction by 2020 may be 14.5%
 74 for sub-Saharan Africa (Lal, 1995). Climate projections of greater rainfall intensity, reduced soil moisture and
 75 increased wind gustiness may cause increases in both wind and water erosion. Increased competition for land is
 76 expected to increase social and political instability, exacerbate food insecurity, poverty, conflict, and migration
 77 (UN-Habitat-GLTN, 2016)

78 To address the threat of land degradation to agriculture, ecosystems and society, in 2015 the United Nations
 79 Convention to Combat Desertification (UNCCD) endorsed Sustainable Development Goal (SDG) target 15.3 – Land
 80 Degradation-Neutrality (LDN), defined as “a state whereby the amount and quality of land resources necessary to
 81 support ecosystem functions and services and enhance food security remain stable or increase within specified
 82 temporal and spatial scales and ecosystems” (UNCCD, 2015). The concept aims to maintain and / or renew the
 83 global resource of healthy and productive land by avoiding, reducing, or reversing land degradation. The complex
 84 interplay between drivers / pressures, degradation processes, the flows for ecosystem services and human needs
 85 and indicators of change are established in the framework (Cowie et al., 2018 see Fig. 3).

86 Three indicators were selected by the UNCCD to evaluate LDN through change in the land-based natural capital:
 87 land cover (metric: physical land cover), land productivity (metric: net primary productivity; NPP) and carbon
 88 stocks (metric: soil organic carbon; SOC). Change in vegetative cover was assumed highly responsive to land use
 89 dynamics e.g., land conversion. Land productivity was selected to represent relatively fast changes in ecosystem
 90 function. Carbon stocks were assumed to represent “...slower changes resulting from the net effects of biomass
 91 growth and disturbance/removal...” and to be used as an indicator of agroecosystem resilience (Cowie et al.,
 92 2018; p. 32). In short, the indicators and associated metrics of ecosystems services are used to monitor neutrality
 93 relative to a baseline and by comparison with gains and losses.

94 The interrelated nature of the LDN indicators, and the role of SOC erosion, can be illustrated with a reduced
 95 complexity framework for estimating change in SOC stocks in ESMs and interpreting measured SOC change (Todd-
 96 Brown et al., 2013). The framework assumes that the soil organic carbon (C_i) pool in area i is at steady state such
 97 that NPP (kg C m^{-2}) inputs equal outputs from heterotrophic respiration (R_i ; kg C m^{-2})

$$98 \quad 0 = \frac{dC_i}{dt} = NPP_i - R_i. \quad (\text{Eq. 1})$$

99 Similarly, it assumes that R_i is directly proportional to C_i with a spatially uniform decomposition rate constant k
 100 (Olson, 1963; Parton et al., 1987)

$$101 \quad R_i = kC_i. \quad (\text{Eq. 2})$$

102 Combining the two above equations produces a model in which C_i is proportional to NPP and inversely
 103 proportional to a global decomposition rate (k)

$$104 \quad C_i = \frac{NPP_i}{k}. \quad (\text{Eq. 3})$$

105 Consistent with Chappell et al. (2015) and others (e.g., Doetterl et al., 2012; Regnier et al., 2013), C_i is also
 106 controlled by wind and water erosion (E_a ; $\text{g soil m}^{-2} \text{ s}^{-1}$) and land cover is one of the main controls on erosion. Land
 107 cover is used in the LDN as a surrogate for erosion. Considering the erosion process, and not just the indicator
 108 land cover, and explicitly accounting for the effects of erosion on SOC stocks, are important because land cover
 109 alone and C budgets used to assess stocks typically do not quantify the erosion impact on the soil resource
 110 (specifically C_i). At best, land cover indicates only that the resource is at risk. By making specific use of land cover
 111 to represent E_a , the framework can be completed:

$$112 \quad C_i = \frac{NPP_i - E_a}{k}. \quad (\text{Eq. 4})$$

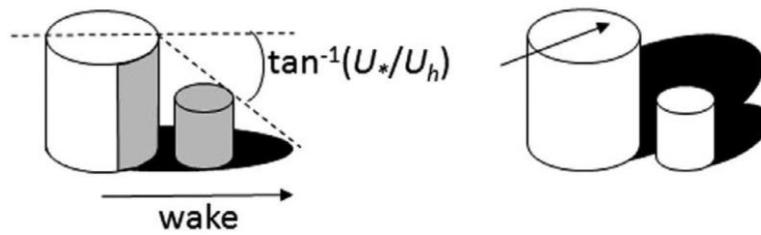
113 The framework demonstrates the interrelated, overlapping nature of the LDN indicators and the critical role
 114 played by E_a . Here, our objective is to show that in global drylands, SOC stocks are reduced rapidly after land use /
 115 land management induced land cover change by wind erosion. We have restricted our estimates of soil erosion to
 116 wind (E) for simplicity and use recent developments of a physically-based sediment transport model to enable

117 consistent global estimation of wind erosion in response to land cover change (Chappell and Webb, 2016). We
 118 show that E provides essential and valuable information about the changing condition of the soil resource and
 119 should be considered formally in assessing C stocks as the basis for evaluating LDN.

120 Methods and Data

121 Wind erosion model

122 Physical land cover is a key indicator of land use, land cover and land management change. Land cover is also one
 123 of the main factors controlling wind erosion and is most easily managed to protect the soil from erosive forces of
 124 the wind. However, land cover itself is not sufficient to explain the occurrence of wind erosion and related
 125 vegetation indices provide only crude approximations for wind erosion assessment (Chappell et al., 2017).
 126 Vegetation structure, density and distribution (width, breadth, height and spacing) plays a critical role in the
 127 protection of the soil from wind erosion and subsequent dust emission. Vegetation extracts momentum from the
 128 wind and shelters downstream areas (behind or in the lee or wake of the vegetation) in proportion to wind speed
 129 (Figure 2).



130 **Figure 2.** The (a) Raupach (1992) concept for reducing the complexity of aerodynamic roughness and its
 131 representation (b) using shadow by Chappell et al. (2010) to enable an approximation from satellite remote
 132 sensing (Figure reproduced from Elsevier journal Remote Sensing of Environment).
 133

134 Chappell and Webb (2016) developed a new approach to wind erosion modelling which established a relation
 135 between sheltered area and the proportion of shadow over a given area; the inverse of direct beam directional
 136 (at-nadir) hemispherical reflectance (black sky albedo; BSA; Chappell et al., 2010). Once normalised by the surface
 137 reflectance properties, ω_{ns} provides the proportion of shadow and has been calibrated against wind tunnel
 138 measurements of several key aerodynamic properties that control wind erosion. For example, Chappell and Webb
 139 (2016) established a strong relation between ω_{ns} and the wind shear stress at the soil surface (u_{s*} ; m s^{-1}) scaled by
 140 freestream wind speed (U_f , m s^{-1} ; Figure 2). These variables drive aeolian sediment transport (Q_h ; $\text{g m}^{-1} \text{s}^{-1}$) for a
 141 given size fraction d :

$$142 \quad Q_h(d) = c \frac{\rho}{g} u_{s*}^3 \left(1 - \left(\frac{u_{*ts}(d)H(w)}{u_{s*}} \right) \right), \quad (\text{Eq. 5})$$

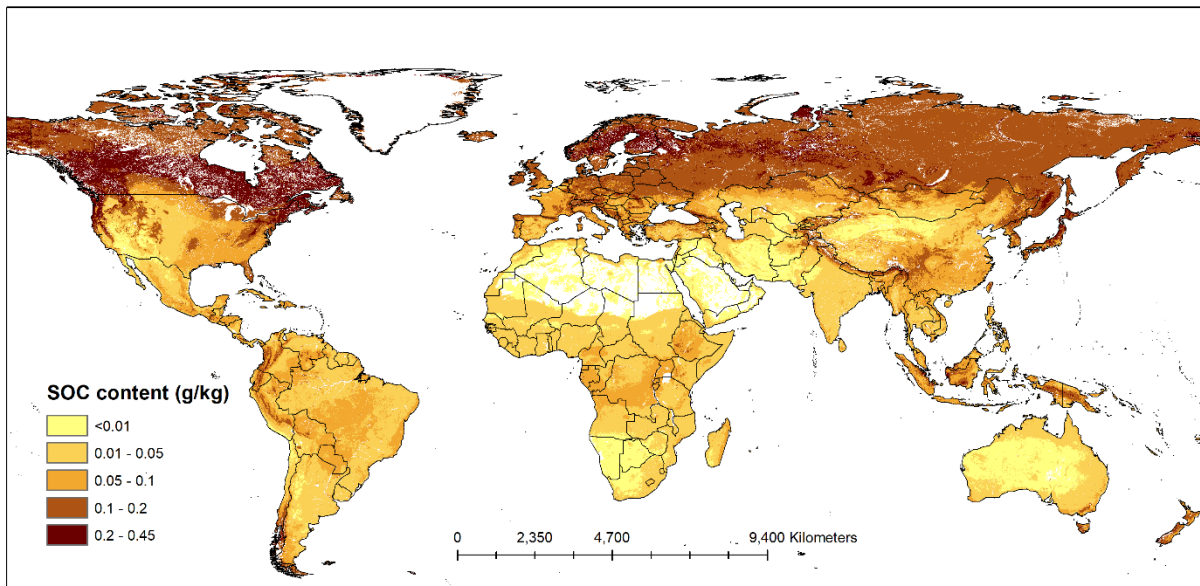
143 where c is a fitting parameter used to adjust the magnitude of the model output, ρ is the density of air (1.23 kg m^{-3}),
 144 g is acceleration due to gravity (9.81 m s^{-2}), u_{*ts} is the soil threshold shear stress of a bare, smooth (no
 145 roughness elements) below which sediment transport does not occur (Shao et al., 1996) and $H(w)$ is a function of
 146 soil moisture which also inhibits transport (Fécan et al., 1999). The model therefore adjusts the total available
 147 wind energy that can be applied to the soil surface u_{s*} by that proportion which exceeds u_{*ts} . Notably, u_{*ts}
 148 provides information on the critical amount of aerodynamic cover required to inhibit wind erosion. Consequently,
 149 it provides valuable information for management.

150 We assumed that the heterogeneity of the transport within the pixel was represented by the albedo of the pixel
 151 and the area of the transport was defined by the pixel. This enabled the transport in one dimension (Q_h ; $\text{g m}^{-1} \text{s}^{-1}$)
 152 to be converted to an areal quantity by dividing by a MODIS pixel side (500 m) to produce wind erosion (E ; $\text{g m}^{-2} \text{s}^{-1}$).
 153 We calculated the amount of SOC removed by wind erosion. Unlike the selective removal of fine, SOC- and
 154 nutrient-rich material by dust emission (Chappell et al., 2013; Webb et al., 2013), we assumed that wind erosion is
 155 not selective. We multiplied E by the number of seconds in one year ($\text{g m}^{-2} \text{y}^{-1}$) and then divided by 100 to convert
 156 the units ($\text{t ha}^{-1} \text{y}^{-1}$).

157 **Model data**

158 The Google Earth Engine (GEE) provides a global geospatial platform for intensive parallel processing of remote
 159 sensing and other environmental data (Gorelick et al., 2017). It currently contains MODIS (MCD43A1, collection 6)
 160 data which provides estimates of land surface albedo at 500 m globally every day for 2000-present. The GEE also
 161 includes the output from numerical weather forecasting and land surface models. Of relevance is the Global Land
 162 Data Assimilation System (GLDAS; Rodell et al., 2004), which provides global wind speed and soil moisture at 25
 163 km resolution every 3 hours for two periods (1948-2010 and 2000-present). The GLDAS ingests satellite and
 164 ground-based observational data products. The GLDAS-2.1 simulation data (2000-present) is forced with National
 165 Oceanic and Atmospheric Administration (NOAA)/Global Data Assimilation System (GDAS) atmospheric analysis
 166 fields, the disaggregated Global Precipitation Climatology Project (GPCP) precipitation fields, and the Air Force
 167 Weather Agency's AGRicultural METeorological modelling system (AGRMET) radiation fields. Using land surface
 168 modelling and data assimilation techniques, it generates optimal fields of land surface states and fluxes (Rodell et
 169 al., 2004).

170 We used existing soil data in the GEE from the SoilGrids dataset (Hengl et al., 2017) to estimate u_{*ts} including soil
 171 texture (clay < 2 μm , silt<50 μm and sand<2000 μm) as a mass fraction at a depth of 0 m and soil organic carbon
 172 (SOC) the mass fraction of carbon by weight in the < 2 mm soil material (Figure 4). This extant global map of soil
 173 organic carbon (SOC) content shows that semi-arid environments particularly around the low latitudes have much
 174 smaller amounts of SOC than other regions. The deserts, displayed in white-yellow, have the smallest SOC stocks.
 175 These regions occur in southern USA and Mexico and across Chile and Argentina. The majority of north Africa has
 176 very little SOC near the surface. A mega-region of small SOC stock occurs across the Arabian Peninsula, through
 177 Iran, China and Mongolia and the majority of continental Australia.



178
 179 **Figure 4.** Predicted soil organic carbon (SOC) content (g kg^{-1}) from the SoilGrids dataset (Hengl et al., 2017).

180 The albedo-based wind erosion scheme above (Chappell and Webb, 2016) was coded in to the GEE making use of
 181 the MODIS albedo, GLDAS wind speed and soil moisture and SoilGrids soil organic carbon content and soil texture
 182 data. These data enable wind erosion estimates to be made at finer spatial and temporal resolution and for time
 183 periods not previously achieved by other schemes. The soil surface shear stress (u_{*s}) was calculated daily 2001-
 184 2016. It is derived from MODIS albedo and influenced by the roughness of all scales (plant canopy, grass coverage,
 185 stone cover, soil aggregates, etc.) which protects the soil surface from wind erosion. We applied the daily MODIS
 186 normalised difference snow index (MOD10A1) to avoid including smooth ice-snow surfaces in the estimates of
 187 wind erosion. We also used daily surface soil temperature to remove situations in which bare but frozen soil
 188 would otherwise contribute to wind erosion. The wind erosion (E ; $\text{t ha}^{-1} \text{y}^{-1}$) was calculated for each pixel every
 189 day between 2001-2016 and the per-pixel mean was calculated and displayed as a map. To establish the SOC

erosion by wind, we multiplied Q_h by the static SOC content (g kg^{-1}), assumed no enrichment of SOC in the eroded material relative to the surface soil, and repeated the procedure as for E .

Calibration data

The aeolian sediment transport model is based on albedo and when calibrated with wind tunnel data provides area-weighted estimates of the driving variable u_{S*} . To calibrate the model, we required consistent areal estimates of transport from measurements taken at many locations (within a study site or pixel). Unfortunately, there are very few area-weighted estimates of sediment transport because of their time-consuming acquisition and a tradition of taking few (often only one) sediment transport samples within a study area. The recently established US National Wind Erosion Research Network tackled this dearth of measurements (Webb et al., 2016). Many samples of sediment transport are collected approximately monthly from selected sites across US agroecological systems. Measurements of horizontal sediment flux (Q_h) were obtained using Modified Wilson and Cooke (MWAC) samplers at the Jornada Experimental Range in New Mexico, USA between June 2015 and December 2017 (Figure 3a). These Q_h measurements were made approximately every month at four heights to 1 m above the soil surface at 27 locations across the measurement area (100 m x 100 m; 1 ha) using stratified random sampling (Figure 3b). This experimental configuration provides an areal (area-weighted) average of the sediment flux which is currently unique in aeolian research monitoring (Webb et al., 2016). The areal Q_h accounts for the spatial distribution in the temporally varying factors which influence wind erosion across the measurement area including variation in vegetation height, spacing and density, soil erodibility, surface shear stress and soil moisture. These measurements of areal Q_h are essential for comparison with the albedo-based estimates of Q_h made over 500 m pixels.

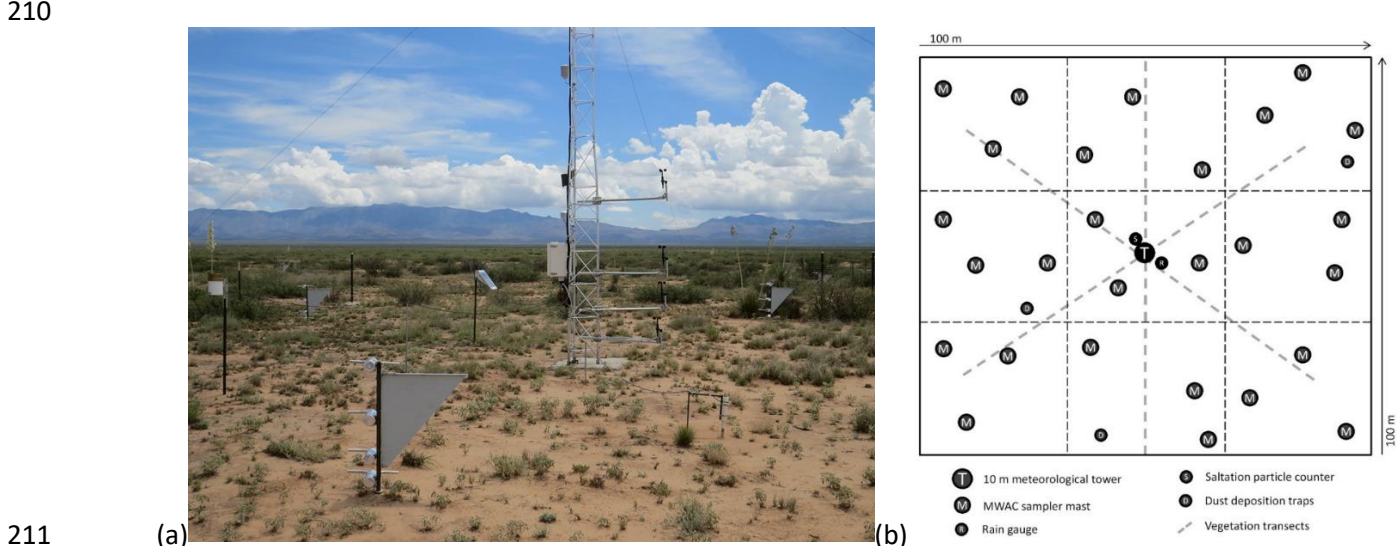


Figure 3. The instrumented site at the Jornada Experimental Range (JER), New Mexico (a) and a schematic representation of the site showing the locations of the Modified Wilson and Cooke (MWAC) sediment samplers and other instruments (b). Taken from the USA National Wind Erosion Research Network (<http://winderosionnetwork.org/>)

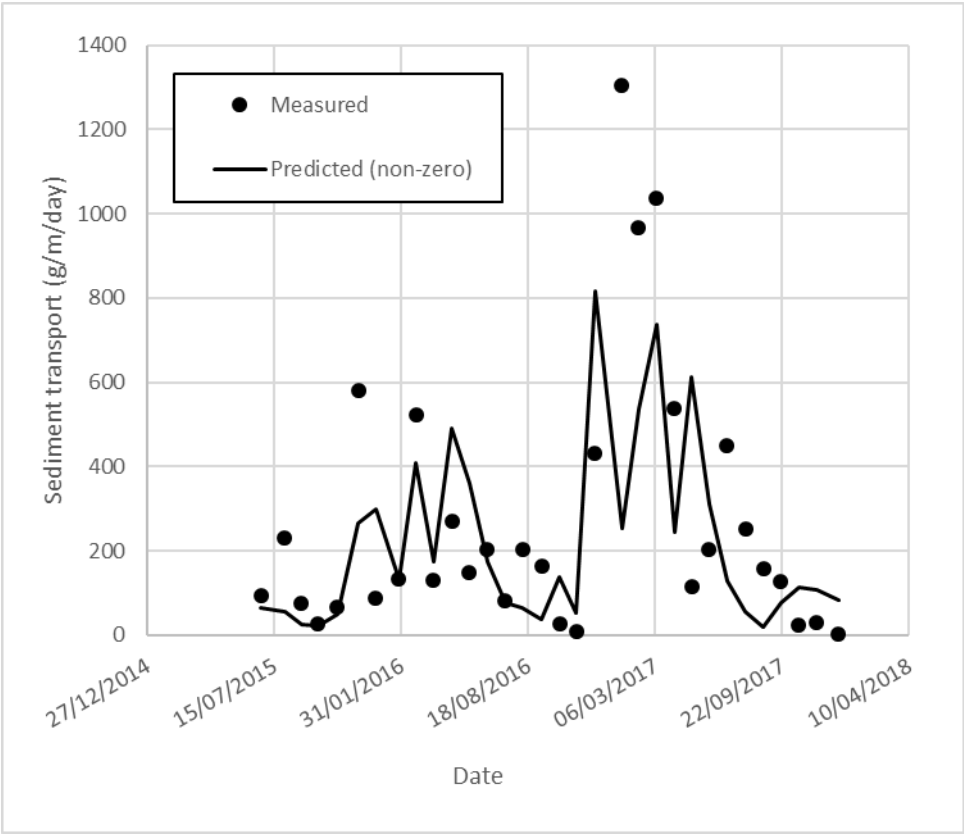
The coordinates of the centre of the JER network site were included in the GEE code. That location was used to identify the 500 m MODIS pixel and to extract for the measurement period the MODIS-based aerodynamic properties. Wind speed (U_h ; m s^{-1}) measurements made at 10 m above ground level at the JER network site were used outside the GEE to make estimates of Q_h using Eq. 1. The predicted Q_h was inverted against the measured Q_h to obtain the optimised value of the parameter c . The value of the parameter that minimised the square root of the mean square error (RMSE) or difference between measured and predicted Q_h , was accepted as optimised.

Results

Sediment transport calibration

Sediment transport was predicted at the JER field site where measurements were made at daily time-steps and then aggregated to approximately monthly intervals which coincided with the measurement intervals. The

227 optimisation of the transport model (Eq. 5) against field measurements produced a RMSE=274 g m⁻¹ month⁻¹ and
 228 showed that the model needs to be adjusted by $c=4.59$ to match the magnitude of measured sediment transport.
 229 Figure 5 shows the time series of measured Q_h at the JER field site and the model estimates using the optimised
 230 parameter values. Small magnitude events are represented by the model, but extremes (at this scale) are less well
 231 represented. It is not clear at this stage whether these extreme amounts of sediment transport originate from the
 232 pixel (autochthonous) or are external to the pixel (allochthonous). In any case, the performance of the model is
 233 adequate; the model predicts at approximately 95% confidence detectable difference in aeolian sediment
 234 transport at 274 g m⁻¹ month⁻¹.
 235
 236



237
 238 **Figure 5.** Time series of horizontal sediment flux (Q_h) measured (black dots) approximately every month between
 239 June 2015 and December 2017. Predictions of Q_h were made every 3 hours for the same period and then
 240 aggregated to match the measurement intervals (black line). The predictions were inverted against the
 241 measurements to optimise the values of the c model parameter.

242 [Global wind erosion and soil organic carbon \(SOC\) loss](#)

243 Figure 6a shows the surface shear stress scaled by freestream wind speed (u_{s^*}/U_f) as a proportion of the
 244 maximum value which provides a measure of how the soil surface is sheltered from the wind. The mean value for
 245 the time period (2001-2016) is different in different regions and under different land use and land cover. The
 246 hyper-arid deserts of North Africa and Middle East have the least sheltering (smoothest surfaces). The next least
 247 sheltered soil surfaces occur across the Earth in North and South America, the Sahelian region of Africa, deserts
 248 through Iran, Afghanistan, the Thar in India and through China and Mongolia and Australia. The most sheltered
 249 surfaces and those least likely to contribute wind erosion are those with <0.5 sheltering. They occur in the main
 250 cultivated regions and forested regions. Where the smoothest, least sheltered surfaces coincide with wind speeds
 251 which exceed the critical threshold (u_{*ts}), wind erosion will occur. Where seasonal variation changes the
 252 aerodynamic roughness e.g., in cultivated regions (across southern Europe, USA and Australia) or land use change
 253 or grazing has changed the vegetation cover (e.g., Amazon rain forest) the soil surface is exposed to wind erosion.

254 We found most wind erosion (E ; t ha⁻¹ y⁻¹) occurs in regions of North Africa, the border between Iran and
 255 Afghanistan and the Gobi Desert of China and Mongolia (Figure 6b). A considerably larger area of intermediate E

256 occurs in the mega-region of drylands through Iran and Afghanistan, the Arabian Peninsula and across northern
257 Africa. Similar magnitude of E is found in the dryland regions of USA and Mexico, Australia and Argentina and
258 Chile. The margins of these regions contain the smallest magnitude of wind erosion but also cover a large area.
259 Since the SOC content of drylands is typically low, the loss of SOC via wind erosion is minimal across most of the
260 vast dryland regions (Figure 6c). However, within all dryland regions there are areas where SOC erosion is much
261 larger. Intermediate SOC erosion occurs in the USA and Mexico and throughout the wind eroded region of
262 southern America and the Sahel. Intermediate values of SOC erosion are also found through Persia and northern
263 China and Mongolia. The largest global SOC erosion by wind occurs in parts of northern and Africa, Somalia and
264 mostly in Mongolia where large SOC content coincides with large wind erosion.

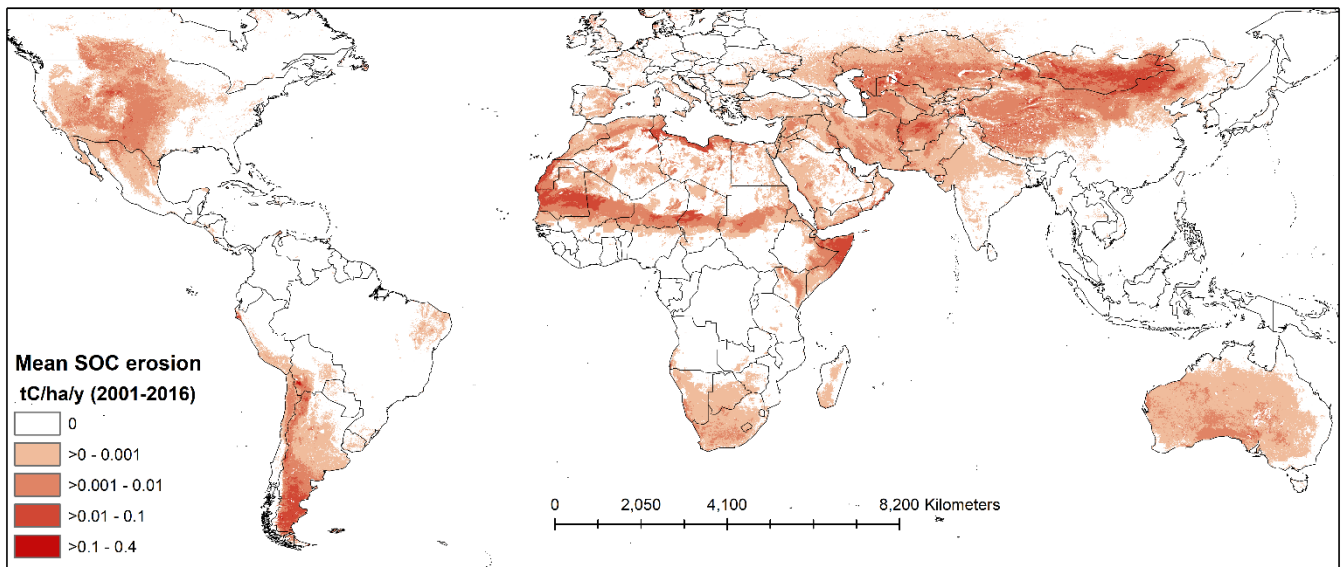
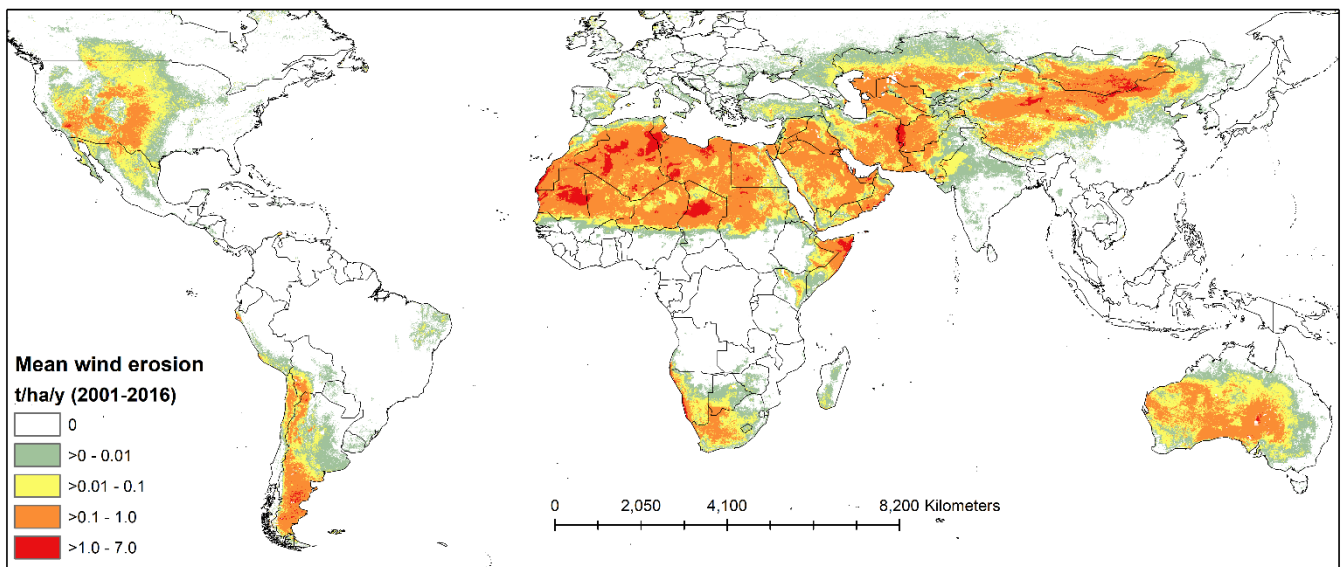
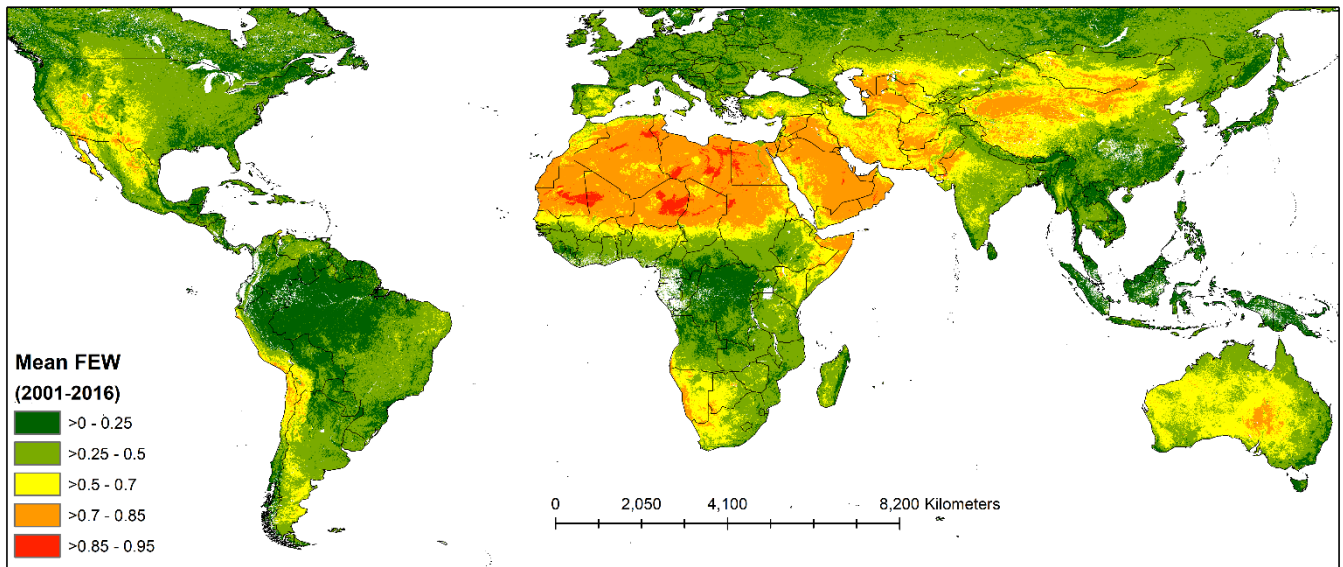
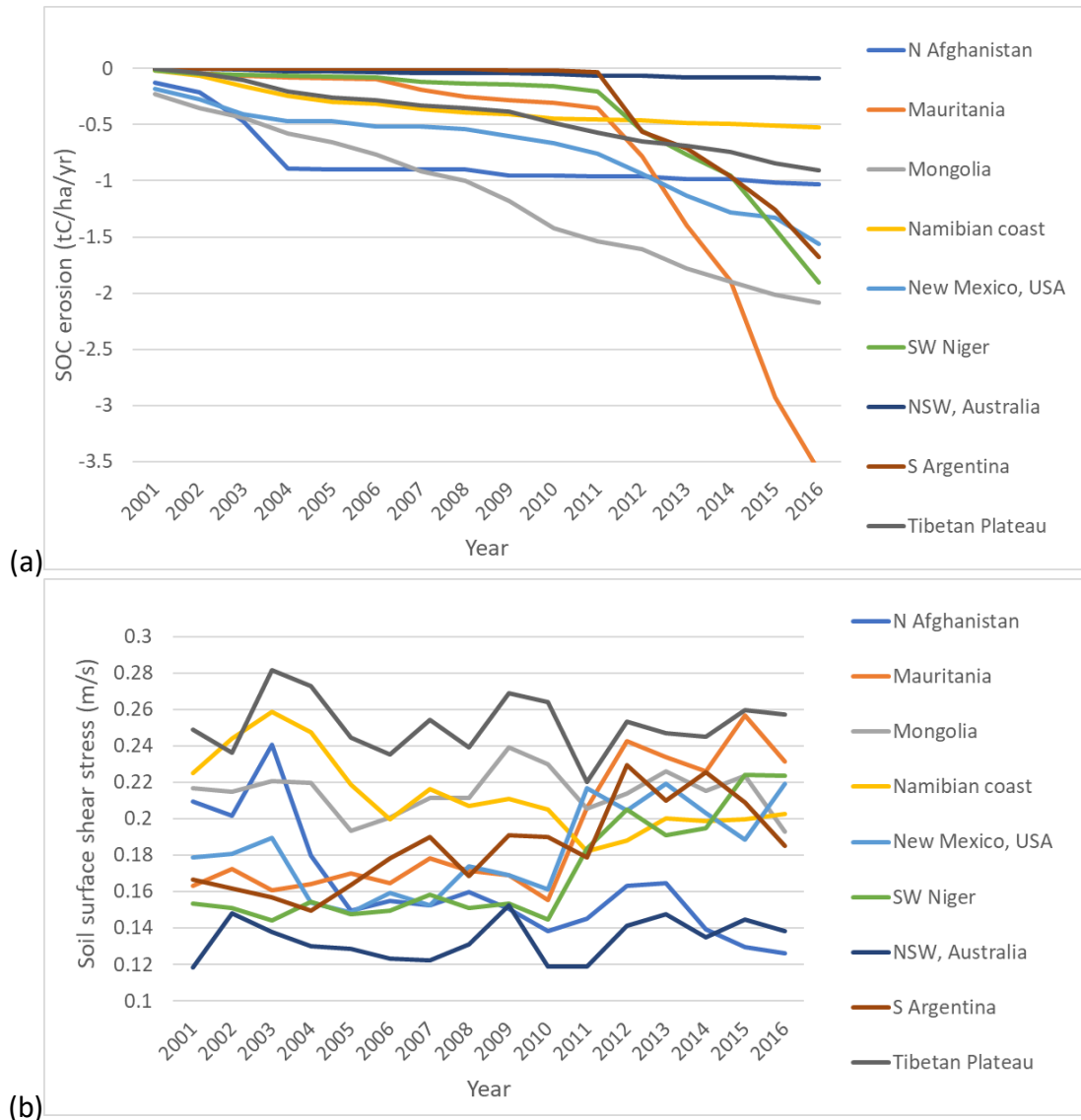


Figure 6. Daily MODIS albedo (500 m; MCD43A1 collection 6), GLDAS (v2.1; 25 km) wind speed and soil moisture and SOC content and soil texture (250 m) data from the SoilGrids dataset (Hengl et al., 2017) used to produce over time (2001-2016) (a) surface shear stress u_{s*} scaled by freestream wind speed (u_{s*}/U_f ; dimensionless) as a

271 proportion of the maximum ($u_{s^*}/U_f=0.04$) which indicates the fraction of erodible soil exposed to wind (FEW; i.e.,
 272 unsheltered); (b) mean annual wind erosion (E ; $t\ ha^{-1}\ y^{-1}$) and (c) soil organic carbon erosion ($tC\ ha^{-1}\ y^{-1}$) by wind.

273 To provide additional insight to the temporal variation of SOC erosion by wind within the global drylands, we
 274 plotted SOC erosion as an accumulation over time for 5 km sites in selected global drylands (Figure 7a). The site in
 275 New South Wales, Australia, is an order of magnitude smaller than other sites and is barely discernible in its
 276 decline. In increasing order of magnitude, the sites in Namibia, the Tibetan Plateau and Mongolia show a linear
 277 rate of declining SOC erosion. In New Mexico, USA the SOC erosion was declining until 2008 and then the rate
 278 increased to 2010 after which it accelerated. Sites in southern Argentina, south-west Niger and Mauritania show a
 279 radical change in SOC erosion after 2010. After 2014 the greatest rate of SOC erosion changed from Mongolia to
 280 Mauritania. The only site to show declining SOC erosion is in northern Afghanistan after 2004.

281



282

283 Figure 7. Selected 5 km sites in global drylands during 2001-2016 showing accumulated soil organic
 284 carbon (SOC) erosion ($tC\ ha^{-1}\ y^{-1}$) removed by wind (a) and change in soil surface shear stress (u_{s^*} ; $m\ s^{-1}$;
 285 b).

286 The cause of these abrupt changes in SOC erosion are due to change in soil surface shear stress by the
 287 balance between changing vegetation cover (represented by FEW) and / or changing wind speed (Figure
 288 7b). The very rapid changes in SOC erosion are very likely to be due to change in wind speed. For
 289 example, the rapid decrease in SOC erosion in northern Afghanistan is very likely due mainly to a
 290 decrease in wind speed. Similarly, the rapid increase in SOC erosion in south-west Niger and Mauritania is
 291 very likely due mainly to an increase in wind speed after 2010. However, the linear increase in u_{s^*} in
 292 southern Argentina and Mongolia is much more likely to be caused by decreasing land surface

293 aerodynamic roughness. Similarly, the linear decrease in u_{s*} on the Namibian coast is more likely to be
294 increasing aerodynamic roughness due to increased vegetation.

295 Discussion

296 Global wind erosion and SOC loss

297 The physically-based wind erosion model enables the identification of global locations where change in surface
298 shear stress (u_{s*}) occurs due to seasonality and land use / land cover changes (Figure 6a). The spatial patterns of
299 u_{s*} for Australia are consistent with those identified nationally by Webb et al. (2006) and across the northern Lake
300 Eyre Basin by Webb et al. (2009) using an empirical land erodibility model. Typically, the largest change in u_{s*}
301 occurs in cultivated regions and exposes the soil to wind erosion. Many of the locations where the largest range in
302 u_{s*} occurs coincide with small wind erosion (Figure 6b). However, rangelands cover a much larger area and have
303 an intermediate range of u_{s*} and the largest wind erosion. Most sediment transport (not dust emission) occurs
304 across North Africa, the Middle East through Iran, Afghanistan and deserts in the China and Mongolia. The
305 majority of extreme wind erosion occur in North Africa with notable exceptions on the border between
306 Afghanistan and Iran and the Gobi desert crossing China and Mongolia.

307 The global cultivated regions have generally small wind erosion but large SOC content and consequently small to
308 intermediate SOC erosion (Figure 6c). The global rangelands have generally intermediate to large wind erosion
309 but small SOC content and consequently intermediate to large SOC erosion. These findings are consistent with
310 those of SOC dust emission for Australia (Chappell et al., 2013). The largest amount of SOC erosion by wind occurs
311 across East Asia and particularly in north-eastern China and Mongolia. Other global 'hot' spots of SOC erosion by
312 wind are Mauritania, Somalia and southern Argentina. Notably, southern USA and Mexico have intermediate
313 wind erosion but large SOC content and consequently SOC erosion in this region is perhaps the second largest
314 global source. The SOC erosion is similar to that of central Asia and the large global area of intermediate SOC
315 erosion by wind which extends across northern China and Mongolia, the Sahel and north African coast, and
316 southern Argentina.

317 The rate of SOC erosion by wind is evident from selected sites in these global drylands (Figure 7). These sites show
318 different rates of SOC removal and some which are accelerating and others which are decelerating. One aspect
319 they have in common is that the SOC erosion is generally rapid. Few field measurements of SOC losses due to
320 wind erosion are available for comparison, although Li et al. (2007) found similarly large rates of SOC erosion due
321 to wind following grass removal in the Chihuahuan desert of southern New Mexico, USA. In our 16-year
322 simulation period, the majority of sites have lost $>1 \text{ tC ha}^{-1} \text{ yr}^{-1}$ by wind erosion and for the same time period in
323 Mongolia the SOC eroded by wind is more than tripled ($>3 \text{ tC ha}^{-1} \text{ yr}^{-1}$). Whilst the SOC content in the surface soil
324 (0-10) may be larger under crops and pastures compared with rangelands, SOC content may be surprisingly large
325 at depth ($>10\text{cm}$), particularly in some drylands. The location of SOC deep ($>10\text{cm}$) in the soil profile may slow
326 decomposition due to limited moisture and nutrients. In these situations, wind erosion and intermediate SOC
327 content will persistently produce large SOC erosion irrespective of the SOC returned to the soil via biomass/NPP
328 (which is comparatively low). Consequently, in these situations SOC erosion will be dependent on the frequency
329 of wind erosion rather than changing stock (with depth, time, productivity) of SOC. It is also possible that SOC
330 erosion rates will decline with time following land cover change as SOC stocks and surface soil textures change.

331 SOC losses from dryland ecosystems and more mesic croplands are likely to have different impacts on the systems
332 depending on the size of SOC stocks, proportional losses of SOC due to erosion, and SOC decomposition and
333 replacement rates (Jackson et al., 2017). Wind erosion of SOC from dryland ecosystems, which have small SOC
334 stocks, may have greater impact on ecosystem function (e.g., soil health and hydrology) and resilience to land
335 management and abiotic drivers of land degradation than in croplands with larger SOC stocks (Lal, 2002). Dryland
336 cropping systems, for example in the Sahel of West Africa, have been found to be particularly susceptible to the
337 impacts of SOC erosion by wind where SOC stocks can be depleted in less than a decade. In Australia, it has been
338 estimated that ignoring SOC erosion increases uncertainty in estimates of C stocks by between 0.08 to 0.27 tC ha^{-1}
339 yr^{-1} (Sanderman and Chappell 2013). This is within the expected SOC sequestration range of some options for

agricultural management (0.11 to 0.75 tC ha⁻¹ yr⁻¹; (Conyers *et al.* 2015)). In these situations, avoided loss of SOC by reducing wind erosion may have more immediate benefits for decreasing land degradation compared with strategies focused on sequestration of SOC.

Global wind erosion model performance

There are no global studies of wind erosion for comparison with our results. However, there are a few regional assessments of wind erosion and many small (field) scale studies using ¹³⁷Cs to estimate medium-term (ca. 30-40 year average) estimates of soil erosion. The challenge with using these studies is that in many dryland regions water erosion may combine with wind erosion to contribute to the measured change in ¹³⁷Cs. Van Pelt *et al.* (2017) used ¹³⁷Cs measurements to partition water erosion and deduce wind erosion of 3.7-6.6 t ha⁻¹ y⁻¹ at an experimental site near Bushland, Texas. At this location our model estimates wind erosion over the 16-year period to be up to 0.1 t ha⁻¹ y⁻¹. Ritchie *et al.* (2003) studied the patterns of soil redistribution in several plant communities in southern New Mexico using ¹³⁷Cs. They found interdune blowout areas representing erosion rates of 3.2 to 4.1 t ha⁻¹ yr⁻¹. Our model estimates of wind erosion were almost the same for that region (1.1 t ha⁻¹ y⁻¹). Our results for North America closely match the spatial patterns of dust-producing regions identified by Prospero *et al.* (2002) and Ginoux *et al.* (2012). Our model includes the Saskatoon region of Canada affected by wind erosion (e.g., Sutherland, 1994).

A recent empirical wind erosion modelling study for Europe shows a very similar pattern to our wind erosion results (Borrelli *et al.*, 2016). Borrelli *et al.* (2016) did not quantify the erosion but the relative magnitude of wind erosion across the wind eroded region of Europe was similar to our results. Notably, our results for wind erosion in the East Anglian region of UK (0.2 6 t ha⁻¹ y⁻¹) were the same order of magnitude as the ¹³⁷Cs-derived estimates of wind erosion (0.6 t ha⁻¹ y⁻¹; Chappell and Warren, 2003).

In western China the Qinghai-Tibetan Plateau is a high altitude arid area that is prone to wind erosion. Yan *et al.* (2001) sampled multiple landforms and land use areas in the north-central and southern part of the region. They determined soil loss rates of 84.1, 69.4, 30.7, and 21.8 t ha⁻¹ yr⁻¹ for shrub-stabilized coppice dunes, semi-stabilized dunes, dryland farm fields, and grasslands, respectively, and for the entire Qinghai-Tibet Plateau, they estimated an annual soil loss rate of 47.6 t ha⁻¹ y⁻¹ (Van Pelt, 2011). These rates are an order of magnitude larger than our findings of 1.6 t ha⁻¹ y⁻¹. In Inner Mongolia, increased grazing pressure increased the susceptibility of the region to wind erosion. Funk *et al.* (2012) used ¹³⁷Cs to estimate wind erosion at 0.5-1.7 t ha⁻¹ y⁻¹ in the valley and windward slope. At the same location our results, albeit for a 16-year period showed wind erosion to be up to 1.3 t ha⁻¹ y⁻¹.

On a transect of Western Australia, Chappell and Baldock (2016) used ¹³⁷Cs measurements across six 50 ha fields and estimated wind erosion at 4.4 ± 2.1 t ha⁻¹ y⁻¹. Our model results for the same locations and part of the same period for wind erosion were up to 0.3 t ha⁻¹ y⁻¹ and for SOC erosion up to 0.003 t C ha⁻¹ y⁻¹. The measured rate had increased relative to an earlier modelled phase suggesting that conservation agriculture had not reduced wind erosion in this region. This study is one of very few which also measured the loss of SOC, reporting up to 0.2 t C ha⁻¹ y⁻¹ had been lost from these fields. Of particular relevance here is that SOC erosion was similar to measured sequestration rates in the region (up to 0.5 t C ha⁻¹ y⁻¹; 10 years) for many management practices recommended for building SOC stocks. Chappell and Baldock (2016) showed that if SOC erosion is equal to (or greater than) the increase in SOC due to management practices, the change will not be detectable (or a loss will be evident). Furthermore, Chappell and Baldock (2016) suggested that "...without including soil erosion in SOC sequestration calculations, the monitoring of SOC stocks will lead to, at best the inability to detect change and, at worst the false impression that management practices have failed to store SOC".

Implications for Land Degradation Neutrality indicators

Land Degradation-Neutrality (LDN) aims to maintain and / or renew the global resource of healthy and productive land by avoiding, reducing, or reversing degradation. By understanding where wind erosion is occurring globally, rather than just where cover is small, land management intervention programs can be prioritised. Because u_{s*} describes the surface roughness, places with stone cover or other non-biotic cover are accounted for in their

extent of protection / sheltering from the wind. By linking wind erosion to SOC, this study shows that SOC stocks are dynamic and threatened by wind erosion in arid drylands. In such areas, the resilience of the soil is under threat and continued wind erosion will compromise their productive potential, ultimately leading to more degraded and retired agricultural land and greater pressure on other areas for production. Consequently, it is feasible to link u_{s*} to an economic assessment e.g., taking in to account how SOC is priced for C sequestration or the cost of using fertiliser to replace soil nutrients removed by wind erosion. Land management decisions that increase u_{s*} , e.g., by increasing grazing intensity and duration and otherwise manipulating land cover, can be directly linked to wind erosion and the economics associated with loss in SOC and soil nutrients. In extensive grazing systems typical of the rangelands, loss of SOC and nutrients can lead to irreversible land use and vegetation change due to the often uneconomic cost of replacing nutrients in these systems. Valuing SOC and nutrients through this approach would enable a full economic costing for the decision-making process.

Some land management practices have caused considerable degradation in some dryland regions. Consequently, it will likely take considerable time to manage degraded lands back to a productive and resilient condition. In other regions where the land is in a desirable condition, the u_{s*} can be used to provide early warning of degradation e.g., during drought or other unforeseen circumstance or highlight those areas at greatest risk of SOC erosion and land degradation. Perhaps most importantly, land managers can set a locally relevant level of u_{s*} for a tolerable amount of wind erosion and establish trigger points for management intervention. Although not shown here, similar global patterns of nitrogen and phosphorous losses are also expected to occur. The patterns are perturbed by small differences in the geographical distribution of nutrient stocks. With tools like the wind erosion model used here, erosion effects on nutrient and SOC stocks could be considered simultaneously in assessments of LDN.

Conclusion

The work presented here provides clear, unambiguous evidence that one of the key indicators for LDN, soil organic carbon (SOC) is declining due to wind erosion:

- 1) SOC does not change slowly from the net effects of biomass and disturbance / removal because SOC can be removed rapidly by wind erosion, particularly after land use and land management induced cover change;
- 2) in the presence of win erosion, SOC cannot be an indicator of resilience because it cannot recover quickly; the SOC erosion is similar to SOC productivity particularly in drylands;
- 3) SOC erosion by wind occurs to a large magnitude in every global region of the vast Earth's drylands (45% of the land surface). The substantial amount of SOC change is negative;
- 4) on these bases, omission of SOC erosion from the LDN framework as a key process would likely cause In accurate assessments of resource condition and highly uncertain policy advice.

We appreciate the LDN indicator of land cover provides a metric of land use effects on ecosystems, e.g., land conversion. Unless these metrics are applied at an appropriate frequency, they will not provide a dynamic response. In contrast, we have shown that by replacing land cover with u_{s*} specific for wind erosion, and then focusing on erosion, we are able to quantify the dynamic impact of a key land degradation process on the soil resource (specifically SOC). Most fundamentally, we have shown that loss of SOC, particularly in drylands, is most likely to be due to wind erosion. Since LDN is focused on maintaining healthy and productive land, and SOC levels are linked to soil health, we believe this approach improves the chances of monitoring and achieving LDN. We recommend that land cover is supplemented with estimates of wind erosion for the global dryland regions of the world due to its dynamic impact on SOC.

Acknowledgements

We are grateful for the resources provided by the Google Earth Engine (GEE) and the technical support of its forum and in particular the help from Noel Gorelick in getting this work coded. We appreciate the GLDAS, MODIS

and SoilGrids data made available via the GEE. Thanks to Stephan Heidenreich for help with the figures and two anonymous reviewers for their comments.

References

- Amundson, R., Berhe, AA., Hopmans, JW., Olson, C., Sztein, AE., Sparks, DL. (2015). Soil and human security in the 21st century. *Science*, 8 May, Vol 348(6235 DOI: 10.1126/science.1261071.
- Bestelmeyer, B.T., Okin, G.S., Duniway, M.C., et al. (2015). Desertification, land use, and the transformation of global drylands. *Frontiers in Ecology and the Environment*, 13: 28-36.
- Chappell A, Warren A. 2003. Spatial scales of ¹³⁷Cs-derived soil flux by wind in a 25 km² arable area of eastern England. *Catena* 52: 209–234. DOI:10.1016/S0341-8162(03)00015-8.
- Chappell, A, Webb NP, Viscarra Rossel RA, Bui E (2014). Australian net (1950s-1990) soil organic carbon erosion: implications for CO₂ emission and land-atmosphere modelling. [Biogeosciences](#), 11, 5235-5244
- Chappell, A. and Webb, N. (2016) Using albedo to reform wind erosion modelling, mapping and monitoring. [Aeolian Research](#) 23, 63–78.
- Chappell, A. and Baldock, J. (2016) Wind erosion reduces soil organic carbon sequestration falsely indicating ineffective management practices. *Aeolian Research* (22): 107-116 10.1016/j.aeolia.2016.07.005
- Chappell, A., Baldock, J., Sanderman, J. (2015) The global significance of omitting soil erosion from soil organic carbon cycling models. *Nature Climate Change* Dec 2015; <http://dx.doi.org/10.1038/nclimate2829>
- Chappell, A., Dong, Z., Van Pelt, S., and Zobeck, T. (2010). Estimating aerodynamic resistance of rough surfaces using angular reflectance. [Remote Sensing of Environment](#), 114 (7): 1462-1470.
- Chappell, A., Webb, N.P., Butler, H. Strong, C. McTainsh, G.H., Leys, J.F and Viscarra Rossel R. (2013) Soil organic carbon dust emission: an omitted global source of atmospheric CO₂. [Global Change Biology](#), 19: 3238–3244.
- Chappell, A., Webb, N.P., Guerschman, J.P., Thomas, D.T., Mata, G., Hancock, R., Leys, J.F., Butler, H. (2017) Improving ground cover monitoring for wind erosion assessment using lateral cover derived from MODIS BRDF parameters. *Remote Sensing of Environment*, <https://doi.org/10.1016/j.rse.2017.09.026>
- Chappell, A., Baldock, M., Gill T.E., Herrick, J.E., Leys, J.F., Marticorena, B., Petherick, L., Schepanski, K., Tatarko, J., Telfer, M., Webb, N.P. 2018. A clarion call for aeolian research to engage with global land degradation and climate change. *Aeolian research* (editorial).
- Conyers M, Liu DL, Kirkegaard J, Orgill S, Oates A, Li G, Poile G, Kirkby C (2015) A review of organic carbon accumulation in soils within the agricultural context of southern New South Wales, Australia. *Field Crops Research* 184, 177-182.
- Cowie, A.L., Orr, B.J., Castillo Sanchez, V.M., Chasek, P., Crossman, N.D., Erlewein, A., Louwagie, G., Maron, M., Metternicht, G.I., Minelli, S., Tengberg, A.E., Walter, S., Welton, S., 2018. Land in balance: The scientific conceptual framework for Land Degradation Neutrality. *Environ. Sci. Policy* 79, 25–35.
- Dialynas YG, Bastola S, Bras RL, Billings SA, Markewitz D, Richter Dd (2016) Topographic variability and the influence of soil erosion on the carbon cycle. *Global Biogeochemical Cycles* 30(5), 644-660.
- Doetterl, S., Van Oost, K. & Six, J. (2012). Towards constraining the magnitude of global agricultural sediment and soil organic carbon fluxes *Earth Surf. Process. Landforms* 37, 642–655.
- Ellerbrock RH, Gerke HH, Deumlich D (2016) Soil organic matter composition along a slope in an erosion-affected arable landscape in North East Germany. *Soil and Tillage Research* 156, 209-218.
- Elliott ET (1986) Aggregate structure and carbon, nitrogen, and phosphorus in native and cultivated soils. *Soil Science Society of America Journal* 50(3), 627-633.
- Faeth, P. & Crosson, P. (1994). Building the case for sustainable agriculture. *Environment*, 36(1): 16-20.
- FAO & ITPS (2015) *The Status of the World's Soil Resources (Main Report)* (Food and Agriculture Organization of the United Nations, Rome, 2015).
- Fecan, F., B. Marticorena, and G. Bergametti (1999), Parameterization of the increase of the aeolian erosion threshold wind friction velocity due to soil moisture for arid and semi-arid areas, *Ann. Geophys.*, 17, 149–157, doi:10.1007/s005850050744.

481 Funk, R., Li, Y., Hoffmann, C., Reiche, M., Zhang, Z., Li, J. and Sommer, M. (2012) Using ¹³⁷Cs to estimate wind
 482 erosion and dust deposition on grassland in Inner Mongolia-selection of a reference site and description
 483 of the temporal variability. *Plant Soil* (2012) 351:293–307. DOI 10.1007/s11104-011-0964-y

484 Ginoux, P., Prospero, J.M., Gill, T.E., Hsu, N.C., Zhao, M. (2012). Global-scale attribution of anthropogenic and
 485 natural dust sources and their emission rates based on MODIS Deep Blue aerosol products. *Reviews of*
 486 *Geophysics*, 50, RG3005.

487 Gorelick, N., Hancher, M., Dixon, M., Ilyushchenko, S., Thau, D., and Moore, R. (2017). Google Earth Engine:
 488 Planetary-scale geospatial analysis for everyone. *Remote Sensing of Environment* (in press).

489 Goudie, A.S., Middleton, N.J., (2006). *Desert Dust in the Global System*. Springer, Berlin, 287 pp.

490 GSP (2017) *Global Soil Partnership Endorses Guidelines on Sustainable Soil Management*
 491 <http://www.fao.org/global-soil-partnership/resources/highlights/detail/en/c/416516/> [Accessed 19 April
 492 2018].

493 Gregorich EG, Greer KJ, Anderson DW, Liang BC (1998) Carbon distribution and losses: erosion and deposition
 494 effects. *Soil and Tillage Research* 47(3–4), 291-302.

495 Hengl, T., Mendes de Jesus, J., Heuvelink, G. B.M., Ruiperez Gonzalez, M., Kilibarda, M. et al. (2017)
 496 SoilGrids250m: global gridded soil information based on Machine Learning. *PLoS ONE* 12(2): e0169748.
 497 doi:10.1371/journal.pone.0169748.

498 Jackson, R.B., Lajtha, K., Crow, S.E., Hugelius, G., Kramer, M.G., Piñeiro, G. (2017). The Ecology of Soil Carbon:
 499 Pools, Vulnerabilities, and Biotic and Abiotic Controls. *Annual Review of Ecology, Evolution, and*
 500 *Systematics* 48: 419-445.

501 Jenny, H. (1941) *Factors of Soil Formation. A System of Quantitative Pedology*. New York: Dover Press. (1994
 502 Reprint, with Foreword by R. Amundson, of the original McGraw-Hill publication)

503 Lal, R. (1990). Soil erosion and land degradation: The global risks. p. 129-172, in R. Lal and BA Stewart (Eds) *Soil*
 504 *degradation*. New York, Springer-Verlag.

505 Lal, R. (1995). Erosion-crop productivity relationships for soils of Africa. *Soil Science Society of America Journal*
 506 59:661-667.

507 Lal, R. (2002). Soil carbon dynamics in cropland and rangeland. *Environmental Pollution* 116: 353-362.

508 Lal R (2003) Soil erosion and the global carbon budget. *Environment International* 29(4), 437-450.

509 Lal R (2004) Soil carbon sequestration impacts on global climate change and food security. *Science* 304(5677),
 510 1623-1627.

511 Lal R (2005) Soil erosion and carbon dynamics. *Soil and Tillage Research* 81(2), 137-142.

512 Leopold, L. 1956. Land use and sediment yield. In: Thomas, W.L. (Ed), *Man's Role in Changing the Face of the*
 513 *Earth*. University of Chicago Press, 639-647.

514 Leys JF, Heidenreich SK, Strong CL, McTainsh GH, Quigley S. 2011. PM10 concentrations and mass transport
 515 during “Red Dawn” - Sydney 23 September 2009. *Aeolian Research* 3, 327-342.

516 Li, J., Okin, G.S., Alvarez, L., Epstein, H., (2007). Quantitative effects of vegetation cover on wind erosion and soil
 517 nutrient loss in a desert grassland of southern New Mexico, USA. *Biogeochemistry* 85: 317-332.

518 Li Y, Yu H, Chappell A, Zhou N, Funk R (2014) How much soil organic carbon sequestration is due to conservation
 519 agriculture reducing soil erosion? *Soil Research* 52(7), 717-726.

520 Li, Y., Zhang, C., Wang, N., Han, Q., Zhang, X., Liu, Y., Xu, L., Ye, W., 2017. Substantial inorganic carbon sink in
 521 closed drainage basins globally. *Nature Geoscience*, 10, 501-506.

522 Luyssaert, S. et al., (2014). Land management and land cover change have impacts of similar magnitude on
 523 surface temperature. *Nature Climate Change*, DOI: 10.1038/NCLIMATE2196.

524 McCarl, B.A., Metting, F.B. and Rice, C. 2007. Soil carbon sequestration. *Climatic Change* 80(1-2), pp.1-3.

525 Mulitza, S., Heslop, D., Pittauerova, D., Fischer, HW., Meyer, I., Stuut, JB., Zabel, M., Mollenhauer, G., Collins, JA.,
 526 Kuhnert, H., and Schulz, M., (2010). Increase in African dust flux at the onset of commercial agriculture in
 527 the Sahel region. *Nature*, Vol 466 doi:10.1038/nature09213.

528 Nguyen B, Lehmann J, Kinyangi J, Smernik R, Riha S, Engelhard M (2008) Long-term black carbon dynamics in
 529 cultivated soil. *Biogeochemistry* 89(3), 295-308.

530 Parajuli, S.P., Zender, C.S. (2017). Connecting geomorphology to dust emission through high-resolution mapping
531 of global land cover and sediment supply. *Aeolian Research* 27: 47-65.

532 Paustian, K., Andr  n, O., Janzen, H.H., Lal, R., Smith, P., Tian, G., Tiessen, H., Noordwijk, M.V. and Woomer, P.L.
533 1997. Agricultural soils as a sink to mitigate CO2 emissions. *Soil use and management* 13(4), pp.230-244.

534 Peters, DPC, Havstad, KM, Archer, SR and Sala, SE (2015). Beyond desertification: new paradigms for dryland
535 landscapes. *Front. Ecol. Environ.*, 13(1): 4–12, doi:10.1890/140276

536 Pimentel, D. (1993). *World Soil Erosion and Conservation*, Cambridge, UK Cambridge University Press.

537 Prospero, J.M., Ginoux, P., Torres, O., Nicholson, S.E., Gill, T.E. (2002). Environmental characterization of global
538 sources of atmospheric soil dust identified with the Nimbus 7 Total Ozone Mapping Spectrometer (TOMS)
539 absorbing aerosol product. *Reviews of Geophysics* 40, 1. doi:10.1029/2000RG000095

540 Raupach, MR, (1992). Drag and drag partition on rough surfaces. *Boundary-Layer Meteorol.* 60, 374–396.

541 Ritchie, J.C., Herrick, J.E., Ritchie, C.A., 2003. Variability in soil redistribution in the northern Chihuahuan Desrt
542 based on 1371489 Cesium measurements. *J. Arid Environ.* 55, 737-746.

543 Rodell, M., P.R. Houser, U. Jambor, J. Gottschalck, K. Mitchell, C.-J. Meng, K. Arsenault, B. Cosgrove, J. Radakovich,
544 M. Bosilovich, J.K. Entin, J.P. Walker, D. Lohmann, and D. Toll 2004. The Global Land Data Assimilation
545 System, *Bull. Amer. Meteor. Soc.*, 85(3), 381-394.

546 Regnier, P., Fridlingstein, P., Ciais, P., Mackenzie, F.T., Gruber, N., Janssens, I.A., Laru-elle, G.G., Lauerwald, R.,
547 Luyssaert, S., Andersson, A.J. (2013). Anthropogenic perturbation of the carbon fluxes from land to ocean.
548 *Nat. Geosci.*, 6, 597–607. <http://dx.doi.org/10.1038/ngeo1830>.

549 Sanderman J, Chappell A (2013) Uncertainty in soil carbon accounting due to unrecognized soil erosion. *Global*
550 *Change Biology* 19(1), 264-272.

551 Shangguan, W., Y. Dai, Q. Duan, B. Liu and H. Yuan (2014), A Global Soil Data Set for Earth System Modeling,
552 *Journal of Advances in Modeling Earth Systems*, 6: 249-263.

553 Singh S, Singh JS (1996) Water-stable aggregates and associated organic matter in forest, savanna, and cropland
554 soils of a seasonally dry tropical region, India. *Biology and Fertility of Soils* 22(1-2), 76-82. [In English]

555 Sommer M, Augustin J, Kleber M (2016) Feedbacks of soil erosion on SOC patterns and carbon dynamics in
556 agricultural landscapes—The CarboZALF experiment. *Soil and Tillage Research* 156, 182-184.

557 Stallard RF (1998) Terrestrial sedimentation and the carbon cycle: Coupling weathering and erosion to carbon
558 burial. *Global Biogeochemical Cycles* 12(2), 231-257.

559 Todd-Brown, KEO, Randerson, JT., Post, WM., Hoffman, FM., Tarnocai, C., Schuur, EAG. and Allison, SD. (2013).
560 Causes of variation in soil carbon simulations from CMIP5 Earth system models and comparison with
561 observations, *Biogeosciences*, 10(3), 1717–1736.

562 UNCCD, 2015. Report of the Conference of the Parties on its twelfth session, held in Ankara from 12 to 23
563 October 2015. Part two: Actions taken by the Conference of the Parties at its twelfth session.
564 ICCD/COP(12)/20/Add. Bonn: United Nations Convention to Combat Desertification.

565 UN-Habitat-GLTN, 2016. Scoping and Status Study on Land and Conflict: Towards UN System-Wide Engagement at
566 Scale. United Nations Human Settlements Programme Report 5/2016.

567 Van Oost K, Quine TA, et al. (2007) The impact of agricultural soil erosion on the global carbon cycle. *Science*
568 318(5850), 626-629.

569 Van Pelt, R.S., Hushmurodov, S.X., Baumhardt, R.L., Chappell, A., Nearing, M.A., Polyakov, V.O., Strack, J.E. (2016).
570 The reduction of partitioned wind and water erosion by conservation agriculture. *Catena*
571 10.1016/j.catena.2016.07.004

572 Webb, N.P., McGowan, H.A., Phinn, S.R., McTainsh, G.H., (2006). AUSLEM (AUStralian Land Erodibility Model): A
573 tool for identifying wind erosion hazard in Australia. *Geomorphology* 78: 179-200.

574 Webb, N.P., McGowan, H.A., Phinn, S.R., McTainsh, G.H., Leys, J.F., (2009). Simulation of the spatiotemporal
575 aspects of land erodibility in the northeast Lake Eyre Basin, Australia, 1980-2006. *Journal of Geophysical*
576 *Research*, Vol. 114, F01013, doi:10.1029/2008JF001097.

577 Webb, N.P., Strong, C.L., Chappell, A, Marx, S.K., McTainsh, G.H., 2013. Soil organic carbon enrichment of dust
578 emissions: magnitude, mechanisms and its implications for the carbon cycle. *Earth Surface Processes and*
579 *Landforms* 38: 1662-1671.

580 Webb, N.P., Herrick, J.E., Van Zee, J.W., Courtright, E.M., Hugenholtz, C.H., Zobeck, T.M., Okin, G.S., Barchyn, T.E.,
 581 Billings, B.J., Boyd, R., Clingan, S.D., Cooper, B.F., Duniway, M.C., Derner, J.D., Fox, F.A., Havstad, K.M.,
 582 Heilman, P., LaPlante, V., Ludwig, N.A., Metz, L.J., Nearing, M.A., Norfleet, M.L., Pierson, F.B., Sanderson,
 583 M.A., Sharratt, B.S., Steiner, J.L., Tatarko, J., Tedela, N.H., Toledo, D., Unnasch, R.S., Van Pelt, R.S.,
 584 Wagner, L., 2016. The National Wind Erosion Research Network: Building a standardized long-term data
 585 resource for aeolian research, modeling and land management. *Aeolian Research* 22, 23-36.
 586 Webb, N.P., Marshall, N.A., Stringer, L.C., Reed, M.S., Chappell, A., Herrick, J.E. (2017). Land degradation and
 587 climate change: building climate resilience in agriculture. *Frontiers in Ecology and the Environments* 15:
 588 450-459.
 589 WHO (2004). *World Health Report*, http://who.int/whr/2004/annex/topic/en/annex_2_en.pdf. (10/1/04) (NB.
 590 Other WHO reports for previous years can be accessed through this site).
 591 Yan, P., Dong, Z., Dong, G., Zhang, X., Zhang, Y., 2001. Preliminary results of using ¹³⁷Cs to study wind erosion in
 592 the Qinghai-Tibet Plateau. *J. Arid Environ.* 47, 443-452.
 593